

V4633 Sgr – a probable second asynchronous polar classical nova

Y. M. Lipkin^{1*} and E. M. Leibowitz^{1*}

¹*School of Physics and Astronomy and the Wise Observatory, Raymond and Beverly Sackler Faculty of Exact Sciences, Tel-Aviv University, Tel Aviv, 69978, Israel*

Accepted 2008 mmmmm dd. Received 2008 February 07; in original form 2008 January 28

ABSTRACT

Photometric observations of V4633 Sgr (Nova Sagittarii 1998) during 1998-2005 reveal the presence of a stable photometric periodicity at $P_1 = 180.8$ min which is probably the orbital period of the underlying binary system. A second period was present in the light curve of the object for six years. Shortly after the nova eruption it was measured as $P_2 = 185.6$ min. It has decreased monotonically in the following few years reaching the value $P_2 = 183.9$ min in 2003. In 2004 it was no longer detectable. We suggest that the second periodicity is the spin of the magnetic white dwarf of this system that rotates nearly synchronously with the orbital revolution. According to our interpretation, the post-eruption evolution of Nova V4633 Sgr follows a track similar to the one taken by V1500 Cyg (Nova Cygni 1975) after that nova eruption, on a somewhat longer time scale. The asynchronism is probably the result of the nova outburst that lead to a considerable expansion of the white dwarf’s photosphere. The increase in the moment of inertia of the star was associated with a corresponding decrease in its spin rate. Our observations have followed the spinning up of the white dwarf resulting from the contraction of its outer envelope as the star is slowly retuning to its pre-outburst state. It is thus the second known asynchronous polar classical nova.

Key words: binaries: close – stars: individual: V4633 Sgr – novae, cataclysmic variables.

1 INTRODUCTION

Nova Sagittarii 1998 was discovered by Liller (1998) on 1998 March 22.4, and reached maximum brightness of 7.4 mag on March 23.7 (Jones 1998). The nova was a fast one, with $t_3 \approx 35$ d in visual and ≈ 49 d in V (Liller & Jones 1999).

In an earlier paper (Lipkin et al. 2001, hereafter L01) we reported on the presence of two photometric signals, early after the eruption: a coherent $P_1 = 3.014$ h periodicity (hereafter the primary signal), and an unstable $P_2 \approx 3.09$ h signal that decreased by 0.3% during three years of observations (hereafter the secondary signal). We suggested that the coherent primary signal is the orbital periodicity of the underlying binary system and that the secondary signal is either superhumps or the spin period of a spinning-up magnetic WD . In the latter interpretation, V4633 Sgr is an asynchronous polar (hereafter, AP) – a strongly-magnetic CV in which the primary’s spin period marginally differs from the orbital period (by $\sim 1\%$, see, e.g., Stauber et al. 2003), and the WD spin-up is caused by the post-eruption contrac-

tion of the strongly-coupled, expanded WD envelope (see Stockman et al. 1988 for a description of the spin dynamics in the prototype, V1500 Cyg).

Preliminary analysis of follow-up observations in 2001-2002 revealed the continued decrease of P_2 , which measured 3.07 h in 2002 (Lipkin & Leibowitz 2004). This further strengthened the asynchronous polar interpretation for the system.

Here we report on the results of observations of two additional years, and on the analysis of our whole accumulated data-set, including a reanalysis of the published data.

2 THE LONG-TERM LIGHT CURVE

The $BVRI$ light curves (LC) of v4633 Sgr accumulated at the Wise Observatory WO during the first 8 yr following its eruption are shown in Fig. 1. These comprise some 16500 images accumulated in 238 nights during 1998-2006. Table 1 summarizes our I -band observations. After the eruption, a 3-yr phase of brightness-decline followed, during which the nova has faded by approximately 8 mag. This initial brightness decline phase ceased in 2001, when a post-nova roughly

* E-mail: yiftah@wise.tau.ac.il (YML); elia@wise.tau.ac.il (EML)

Table 1. A summary of the *I*-band observations of V4633 Sgr (note that in 2006 only a few *B* and *R*, but no *I* snapshot were observed)

Year	1998	1999	2000	2001	2002	2003	2004	2005
Images	4035	2103	1205	2317	1083	1226	683	1
Nights	33	34	38	58	28	20	12	1

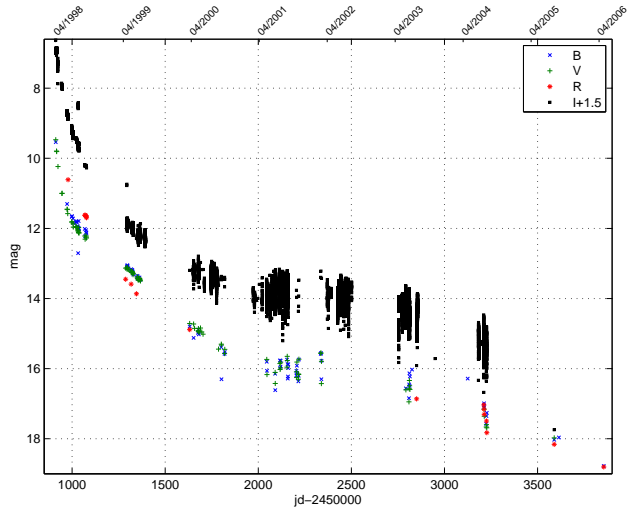


Figure 1. The *BVRI* LCs of V4633 Sgr in 1998-2006. The *BVR* plots are nightly averages of our observations, while the *I* plot is our full data. The *I* LC is shifted up by 1.5 mag for better viewing.

stable brightness state of 15.5-16 mag has been reached. In 2003, a new phase of brightness-decline commenced, and the system faded during the following 4 years by ~ 3 mag to 18-19 mag in 2006 at the end of our observations.

3 THE PRIMARY SIGNAL

Figure 2 shows a periodogram of the 1999-2004 *I*-band LC of V4633 Sgr. The periodogram shows the χ^2/dof values obtained by fitting the data to a sine wave with test-frequencies spanning the range shown in the figure, and to a 7th-degree polynomial, introduced to detrend the post-eruption secular brightness decline of the nova. The periodogram is dominated by the peak of the primary signal at 7.964 d^{-1} (marked by a solid-line arrow in Fig. 2) and its complex alias structure, affirming the coherence of this signal over the time spanned by our observations. The second harmonic of P_1 at twice the fundamental frequency, 15.928 d^{-1} , is also clearly present in the periodogram (marked by a dashed-line arrow in Fig. 2). The best-fit value of the fundamental frequency is $P_1 = 180.8169 \pm 0.0002 \text{ min}$ (the quoted error is $1\text{-}\sigma$ confidence level that was derived by a sample of 3000 bootstrap simulations, Efron & Tibshirani 1993). This result is insensitive to the degree of polynomial used to detrend the LC, for 6th- to 11th-degree polynomials. The calculated eperemeris of the primary minima is given in Equation 1.

$$\text{HJD } T_{\min} = 2453227.59405596 + 0.125567(27)E \quad (1)$$

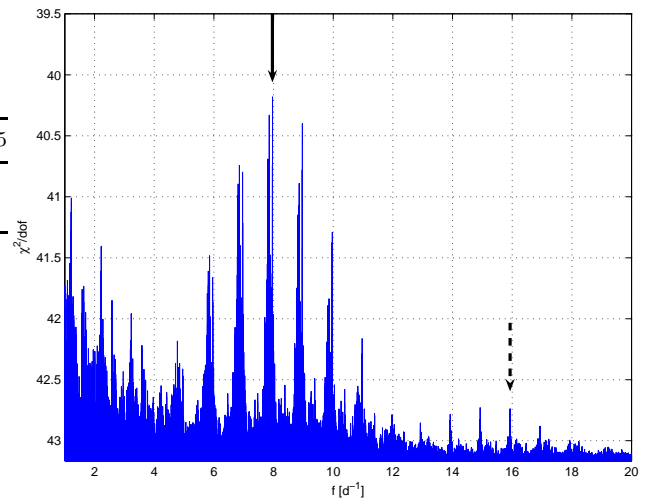


Figure 2. A Periodogram of the 1999-2004 *I*-band data of V4633 Sgr. The y-axis is the χ^2/dof obtained by fitting the data to a 7th-degree polynomial and a sine wave with test frequencies spanning the range shown in the figure. The y-axis is flipped so that better-fitting frequencies (lower χ^2/dof) are peaks instead of troughs. The best-fitted frequency at 7.964 d^{-1} is marked by a solid-line arrow. The second harmonic, at 15.928 d^{-1} is marked by the dashed-line arrow.

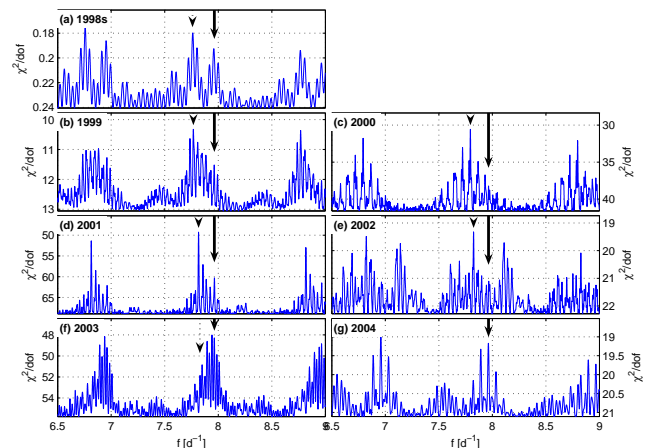


Figure 3. Yearly periodograms of V4633 Sgr, obtained by fitting each yearly data to a 3rd-degree polynomial and a sine function with a test frequency. The primary signal is marked in each plot by a solid-line arrow, and the secondary signal is marked by a dashed-line arrow.

Measurements of P_1 in each observational season are also consistent with a stable period (the yearly measurements are presented as the P'_1 column in Table 2; the upper limit for variation of P_1 is $\dot{P}_1 \leq 1.1 \times 10^{-8}$).

Periodograms of each observational season are shown in Fig. 3. Each data-set was fitted to a sine function and a 3rd-degree polynomial. The primary signal is clearly present in each of the periodograms (marked by a solid-line arrow), and is the prominent signal in the periodograms of 2003 and 2004.

The yearly waveforms of P_1 are shown in Fig. 4. In each case, the LC was detrended prior to folding by subtract-

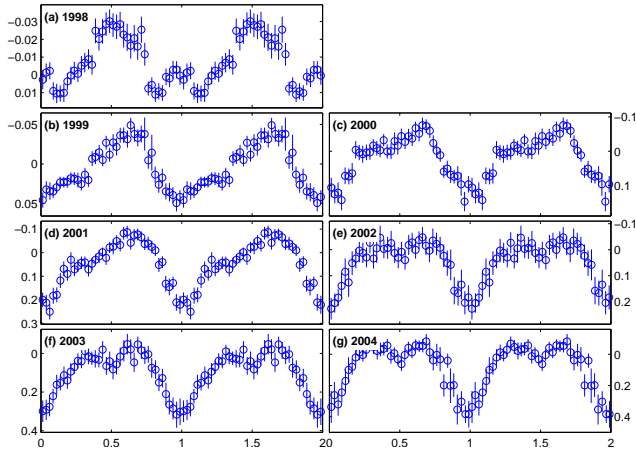


Figure 4. The I LCs of each of the observational seasons folded on the period of P_1 . Discrete points are mean magnitudes in each of 40 equal bins covering the 0–1 phase interval. The inserted bars are the standard deviation in the value of the mean in each bin. In all but the 2004 data, the signal of P_2 and a 3rd-degree polynomial were subtracted prior to folding. Note the difference in the y-axis scales.

ing the secondary signal and a 3rd-degree polynomial (see Sec. 4). The initial waveform of P_1 in 1998 was symmetric around a single major minimum. A clear small symmetric hump of short duration is seen at the center of this minimum, indicating a slight brightening of the system around the phase of lowest point. In the following year the minimum became asymmetric around the low point, with a slow rise and a fast decline. It then gradually turned more symmetric, with a primary minimum and a secondary dip of 0.1233 mag in 2004. Note that the primary minimum of this periodicity preserved its phase throughout the 8 years of our observations. If it is the phase of superior conjunction of the WD, the 1998 profile indicates that shortly after outburst, namely within a few tens of days following the eruption, there was a particular intense activity in the system, either on the surface of the WD or in its close vicinity, that took place along the interbinary center line.

The full amplitude of P_1 in 1998–2004 was 0.040 mag, 0.085 mag, 0.20 mag, 0.30 mag, 0.26 mag, 0.36 mag, and 0.45 mag in each of the years, respectively. The flux variation of P_1 in 1999–2004 relative to that of 1998 was 0.085, 0.069, 0.068, 0.055, 0.048, and 0.028, respectively.

4 THE SECONDARY SIGNAL

We tested the yearly light curves for a second signal by fitting each data-set to a 3rd-degree polynomial, the first three harmonics of P_1 , and a sine function with test-frequencies spanning the range 5 d^{-1} – 12 d^{-1} . The resulting periodograms (hereafter, the secondary periodograms) are shown in Fig. 5. The strongest signal in each periodogram, which is the secondary signal in the LC, is marked by a solid-line arrow. The dashed arrow marks the frequency of P_1 .

In the primary, as well as in the secondary periodograms of the data-sets of the first five years, 1998 – 2002, the prominent peak corresponds to a period P_2 that is slightly longer

Table 2. The best-fit values of the primary and the secondary signals in each observational season. The second column (P_2) presents the results for P_2 when $P_1 = 180.8169 \pm 0.0002$ min, the best fit value for the entire LC, was set fixed. The third and fourth columns (P'_1 and P'_2) are the results for P_1 and P_2 when both signals were fitted simultaneously (see text for a full description).

Year	P_2 [min]	P'_1 [min]	P'_2 [min]
1998	185.577 ± 0.038	180.711 ± 0.081	185.604 ± 0.039
1999	185.394 ± 0.007	180.852 ± 0.008	185.396 ± 0.006
2000	184.738 ± 0.005	180.817 ± 0.009	184.739 ± 0.005
2001	184.239 ± 0.004	180.808 ± 0.007	184.238 ± 0.004
2002	184.033 ± 0.009	180.768 ± 0.011	184.045 ± 0.009
2003	183.946 ± 0.018	180.838 ± 0.009	183.945 ± 0.014
2004	-	180.846 ± 0.027	-

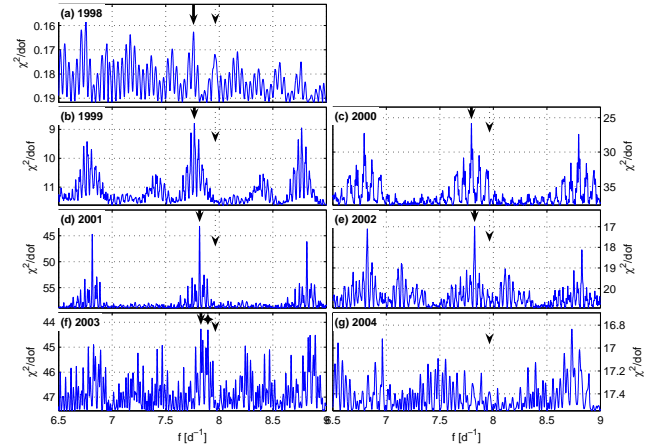


Figure 5. The same as Fig. 3; Each yearly data-set was fit to a 3rd-degree polynomial, the first three harmonics of P_1 , and a sine wave. In each periodogram, the frequency of the primary signal is marked by a dashed-line arrow, and the secondary signal by a solid-line arrow. The secondary signal is not detectable in the 2004 periodogram

than P_1 (in 1998 it is the 1-day alias of what we consider the true periodicity in the LC). The best-fit values of P_2 in each yearly data-set are given in Table 2 (Col. 2). The secondary period monotonically decreased at a rate that also declined. It was 2.6% longer than P_1 a few months after the eruption, becoming 1.8% longer than P_1 four years after. Consistent results are obtained when each yearly data-set is fit simultaneously to P_1 and P_2 (Table 2, Col. 4), or by conducting the analysis using different parameters (a lower degree polynomial, fewer harmonics of P_1 , or more harmonics of the test frequency).

The secondary periodogram of 2003 features a prominent signal at 7.83 d^{-1} , 1.7% longer than the primary signal, which we identify as the still-declining P_2 . A slightly lower peak at 7.89 d^{-1} (marked with a star-headed arrow in Fig. 5) is probably an alias.

The yearly waveforms of P_2 are shown in Fig. 6. The LCs were detrended prior to folding by removing P_1 and a 3rd-degree polynomial. The full amplitude of P_2 was

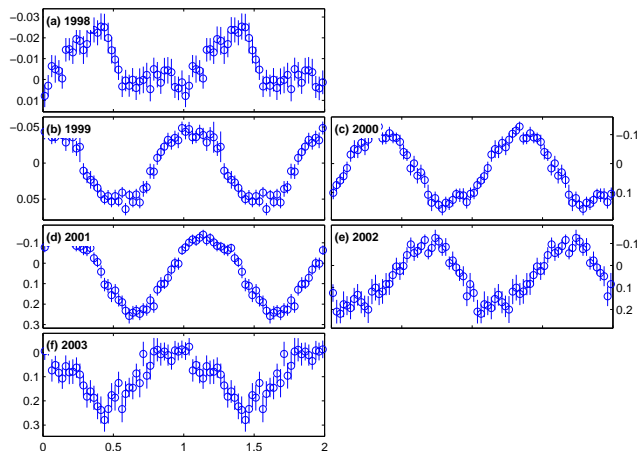


Figure 6. The same as Fig. 4, with the LCs folded on the period of P_2 .

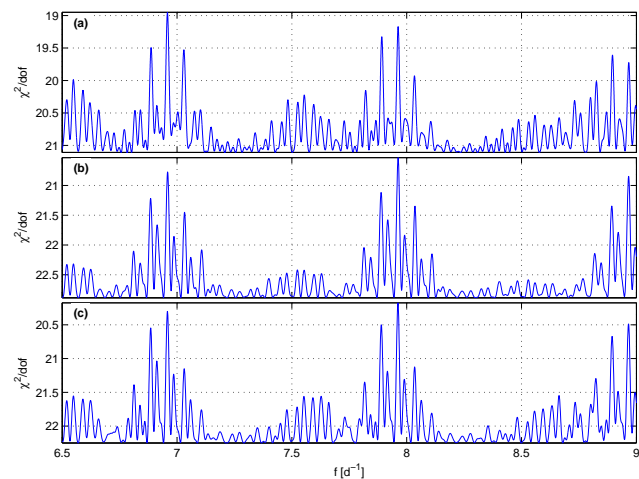


Figure 7. (a) The same as Fig. 3 (g). (b) A periodogram of an artificial LC of 2004, consisting of the fitted polynomial and signal of P_1 , and randomly-selected residuals. (c) A periodogram of an artificial LC of 2004, consisting of the fitted signals of P_1 and the 9.73 periodicity, a polynomial, and randomly-selected residuals. The periodograms of the artificial sets were derived in the same way as the periodogram of the actual data.

0.03 mag, 0.11 mag, 0.29 mag, 0.40 mag, 0.34 mag, and 0.30 mag, in 1998–2003, respectively.

The 2004 secondary periodogram shows no significant signal in the expected frequency range of P_2 . The most significant frequency in the 6 d^{-1} – 10 d^{-1} is at 9.73 d^{-1} , the one-day alias of which at 8.73 is marked in Fig. 5. Its $\frac{1}{2}$ day alias at 7.73 d^{-1} is the most significant peak in the 7.7 d^{-1} – 7.9 d^{-1} range, where P_2 is expected. To confirm the absence of the secondary signal from the 2004 data, we constructed an artificial LC of 2004 consisting of the best-fitting primary signal and a polynomial, to which we randomly added the residuals between the fitted and the observed data. The periodogram of the artificial LC is very similar to that of the observed one (Fig. 7, top and center panels). Another artificial data-set, that also comprises the fitted 9.73 signal yielded similar results (Fig. 7, bottom panel).

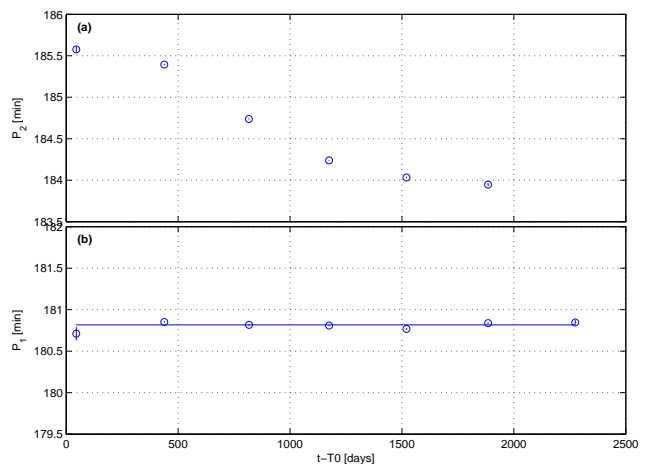


Figure 8. The two signals in 1998–2004. The x-axis is the time since the nova eruption. The vertical lines crossing the circles are the error bars. The time evolution of P_2 is shown in the top panel. The bottom panel shows the measured yearly values of P_1 . The solid line is the best-fitted value of P_1 in 1999–2004

5 DISCUSSION

The analysis of 8-year data of V4633 Sgr allows us to review and refine the main results presented in L01, as well as to follow the continued post-eruption evolution of the nova. We confirm the presence of two independent signals in the data, as found by L01. Both signals were present in the LC some 41 days after the eruption, and possibly earlier.

The primary signal was detectable in all of the time-resolved data-sets that followed, the latest of which was in 2004 August. The period of the primary signal was confirmed to be stable over the time base of our observations, (see Table 2 and Fig. 8, lower panel), and coherent over the 5.3 yr time-base in which its coherence was tested for. These characteristics support the interpretation of L01 for this signal as the orbital period of the underlying binary system. The long time-base of the observations allowed us to refine the period of the primary signal, $P_1 = 180.8169 \pm 0.0002 \text{ min}$. The waveform of P_1 , having an initial symmetric and then asymmetric saw-tooth shape, had evolved into a symmetrical form with primary and secondary lows. These changes may reflect the changing geometry of the binary (e.g., the contraction of the swollen primary), and changes in the relative brightness of the system components.

The secondary signal, which was found to vary by L01, has decreased monotonically by 0.9% following the eruption, from being 2.6% longer than P_1 some 40 days after the eruption, to 1.7% longer five years later. (Table 2 and Fig. 8, upper panel). In 1999–2003, the period decline-rate was also reduced monotonically by an order of magnitude (from $\dot{P}_2 \approx (-1.203 \pm 0.016) \times 10^{-6}$ in 1999–2000 to $\dot{P}_2 \approx (-1.7 \pm 0.4) \times 10^{-7}$ in 2002–2003). Finally, the secondary signal was undetectable in the data in 2004.

L01 proposed two possible interpretations to the secondary signal: a permanent superhump, and more likely, the spin period of a magnetic *WD* of an asynchronous polar system. Our results further weaken the permanent superhump interpretation. The continued decline of P_2 further lowers the upper limit of the secondary mass estimated by L01,

thus requiring an exceptionally under-massed secondary, and an extremely evolved CV system to be accounted for (L01 Sec. 4.5 and references therein). Moreover, the monotonic decrease of P_2 over a 5 yr time span is atypical for a permanent superhump signal, which is expected to wander randomly about a mean period that is determined by the mass-ratio of the system.

Our results further support the AP model. In particular, the post-eruption evolution of V4633 Sgr bares some remarkable similarities to that of V1500 Cyg (Nova Cygni 1975) – the AP prototype, and one of the fastest and brightest novae of the 20th century ($t_2 = 2.43$ d, $m_{V,max} = 1.85$, Young et al. 1976).

Nova Cygni displayed some unique photometric features following its eruption. A few days after outburst, a periodic variation, $\sim 1\%$ longer than the $P_{orb} = 201$ min orbital period, was detected, initially in the profiles of emission lines, and shortly after also photometrically (Patterson 1978; note that the photometric orbital modulation became detectably in photometry only 2 years after the eruption). In the following 10 days or so, the period decreased by $\sim 1\%$, synchronizing with the orbital period. The period continued to decrease by an additional $\sim 1\%$ during the following year or so, after which the variation disappeared. The periodicity, with a marginally shorter period, was rediscovered some 10 yr later in the modulation of the optical circular polarization (Stockman et al. 1988), having an increasing trend, with $\dot{P} = 4.4 \times 10^{-8}$ (Schmidt & Stockman 1991).

The polarized periodicity was naturally associated with the spin of a strongly magnetic *WD*, which in turn implied that the early photometric variation was a tracer of the *WD* spin evolution following the nova eruption. The commonly accepted scenario of this evolution was sketched by Stockman et al. (1988). They proposed that prior to the eruption, V1500 Cyg was an ordinary, synchronized polar. The rapid expansion of the strongly-coupled *WD* envelope due to the nova explosion increased the primary’s moment of inertia, which lead, owing to the conservation of angular momentum, to the *WD* spin-down by $\sim 1\%$. Strong magnetic coupling between the secondary and the expanded envelope during the first few days after the eruption lead to a phase of extremely rapid spin-up (with $\dot{P} \sim 10^{-4}$), which resulted in the resynchronization of the *WD* spin and the orbital period. The contraction of the remnant envelope onto the *WD* surface over the next year or so lead to a second spin-up phase, at a rate that is slower by two orders of magnitude. The photometric spin signal was switched off when the envelope finally collapsed onto the *WD* surface and residual nuclear burning ceased. The spin-down, with a synchronization time scale of ~ 150 yr, which was observed in polarimetry more than a decade later was naturally interpreted as a magnetically-driven synchronization.

V4633 Sgr shares some striking observational similarities with V1500 Cyg. Shortly after their eruption, both novae exhibited a periodicity that was slightly longer (by $\sim 1\%$ - 2.6%) than the orbital period (in V1500 Cyg within a week, and in V4633 Sgr after ~ 40 d).

In both systems the signal’s period decreased monotonically at a rate of $\dot{P} \sim 10^{-6}$ that declined with time (the second spin-up phase of V1500 Cyg). Finally, in both cases the unstable signal disappeared a short time after the erup-

tion (~ 1.5 yr and ~ 5.2 yr, in V1500 Cyg and V4633Sgr, respectively).

These similarities in the post-eruption evolution of V1500 Cyg and V4633 Sgr further support the AP model that was proposed by L01 for the latter. Applying this model to V4633 Sgr, and assuming a post-eruption evolution similar to that of V1500 Cyg, we note a number of differences between the two systems. The earliest measurement of the *WD* spin of V4633 Sgr, some 40 days after the eruption, yielded a spin period longer than P_{orb} by $\sim 2.6\%$ – about twice the difference measured in V1500 Cyg shortly after its eruption – implying either a greater loss of angular momentum in the eruption of V4633 Sgr, or a greater increase of the *WD* moment of inertia. This would require either a stronger magnetic field, which would have coupled the ejecta over a longer distance, and/or more mass ejected during the eruption. We note that because the brightness decline-rate of V4633 Sgr ($t_3 \approx 42$ d) was longer than in V1500 Cyg, the former’s *WD* should be less massive (L01, Sec. 4.3 and references therein), and is therefore expected to eject more mass (Yaron et al. 2005).

An extremely-rapid spin-up phase which was observed during the first dozen days or so following the V1500 Cyg nova eruption was not observed in V4633 Sgr, and particularly, no early resynchronization has occurred. As a result, the *WD* spin period is longer than P_{orb} in V4633 Sgr, whereas in V1500 Cyg it is shorter. The lack of early resynchronization implies that either the strong coupling between the secondary and the envelope that was proposed by Stockman et al. (1988) for V1500 Cyg was considerably weaker in V4633 Sgr. Alternatively, if a rapid spin-up did occur, the desynchronization of the *WD* during the eruption of V4633 Sgr must have been significantly stronger, implying a much greater loss of angular momentum during the nova eruption.

The *WD* spin period decreased over the 5 yr following the eruption by 0.9% – similar to the period decrease in the second spin-up phase of V1500 Cyg. If we naively assume an even-density contracting envelope surrounding a *WD*, a strong *WD*-envelope coupling that effectively causes a rigid-body behavior, angular-momentum conservation, and a 10^{-5} - $10^{-6} M_{\odot}$ envelope, the observed ΔP_{rot} would require an initial $(30-100)R_{WD}$ envelope – a reasonable figure in the framework of the Stockman et al. (1988) model.

Finally, the envelope-contraction phase lasted ~ 5.28 yr in V4633 Sgr – more than 4 times longer than in V1500 Cyg. As pointed out by L01, the longer envelope-contraction time-scale also is expected for the less massive *WD* (Yaron et al. 2005; note however that analysis of *XMM-Newton* observations by Hernanz & Sala 2007 suggests that nuclear burning turned off less than 2.5 yr after the outburst).

The brightness modulation over the spin period suggests an intrinsic brightness source on the *WD* surface, which is non-uniformly distributed. The turning off in 2004 of this considerable source ($\sim 25\%$ of the total brightness in 2003) may account for the renewed fading of the system, perhaps because of reduced accretion due to decreased irradiation of the secondary. The source of the non-uniform brightness may be a hot spot due to enhanced nuclear burning near the *WD* accreting pole, as suggested by Stockman et al. (1988) for V1500 Cyg. This would naturally account for the early appearance of the spin modulation, less than 1.5 months af-

ter the eruption. The disappearance of the signal 5 yr later may also be easily explained by the final collapse of the envelope, and the termination of the nuclear burning.

The contracting envelope – the driving mechanism of the *WD* spin up, may also have contributed a significant fraction of the primary’s brightness variation. Let us once again naively assume a *WD* surrounded by an even-density contracting envelope with a mass $M_{env} = \alpha M_{WD}$ ($\alpha \approx 10^{-5}-10^{-6}$) and an initial post-eruption radius of $R_{env} = \beta R_{WD}$ ($\beta \approx 30-100$), a strong *WD*-envelope coupling leading to a rigid-body behavior, and angular-momentum conservation. The initial energy is the sum of the kinetic energy:

$$E_{K0} = \frac{1}{2}(I_{wd} + I_{env})\omega_0^2 \approx \frac{1}{2}I_{wd}\frac{\omega_f}{\omega_0}\omega_0^2 = \frac{1}{2}I_{wd}\omega_f\omega_0,$$

and the gravitational energy:

$$\begin{aligned} U_0 &= - \int_{R_{wd}}^{R_{env}} \frac{GM_{wd}M_{env}(r)}{r} dr \approx \\ &= -2\pi GM_{wd} \frac{M_{env}}{\frac{4\pi}{3}(R_{env}^3 - R_{wd}^3)} (R_{env}^2 - R_{wd}^2) = \\ &= -\frac{3}{2}GM_{wd}M_{env} \frac{R_{env}^2 - R_{wd}^2}{R_{env}^3 - R_{wd}^3} = -\frac{3GM_{wd}^2}{2R_{wd}} \alpha \frac{\beta^2 - 1}{\beta^3 - 1}, \end{aligned}$$

where ω_0 and ω_f are the initial and final *WD* angular velocities, and $\frac{\omega_f - \omega_0}{\omega_0} \approx 2.6\%$. The final energy is:

$$E_{Kf} + U_f \approx \frac{1}{2}I_{wd}\omega_f^2 - \frac{GM_{wd}M_{env}}{R_{wd}} = \frac{1}{2}I_{wd}\omega_f^2 - \alpha \frac{GM_{wd}^2}{R_{wd}},$$

and the energy released during the envelope contraction is:

$$\begin{aligned} \Delta E &\approx \frac{1}{2}I_{wd}\omega_0^2 \left(1 - \frac{\omega_0}{\omega_f}\right) - \alpha \frac{GM_{wd}^2}{R_{wd}} \left(1 - \frac{3}{2} \frac{\beta^2 - 1}{\beta^3 - 1}\right) = \\ &= \frac{1}{5}M_{wd}R_{WD}^2\omega_0^2 \left(1 - \frac{\omega_0}{\omega_f}\right) - \alpha \frac{GM_{wd}^2}{R_{wd}} \left(1 - \frac{3}{2} \frac{\beta^2 - 1}{\beta^3 - 1}\right). \end{aligned}$$

Inserting typical *WD* mass and radius, α and β , we obtain:

$$\begin{aligned} \Delta E &\approx 1.4 \cdot 10^{40} \text{ erg} - \alpha \left(1 - \frac{3}{2} \frac{\beta^2 - 1}{\beta^3 - 1}\right) 3.8 \cdot 10^{50} \text{ erg} \approx \\ &\approx -10^{44-45} \text{ erg} \end{aligned}$$

These order of magnitude calculations show that only a marginal fraction of the gravitational energy release that is associated with the contraction of the envelope is required for the spinning up of the *WD*. Almost all of it, an amount of energy sufficient to maintain an Eddington luminosity of $10^{38} \text{ erg s}^{-1}$ for for 0.1-1 years, is radiated away during the envelope’s contraction. Because of the strong magnetic field of the *WD* that couples it, the hot, ionized envelope cannot contract radially, but is forced to accrete along the magnetic-field lines towards the magnetic poles of the *WD*. It is thus reasonable that most of this energy is released near the magnetic poles, becoming a major energy source for a hot spot near one or the two poles, and a significant fraction of the variable brightness component on the white dwarf (and indeed, of total luminosity of the system) during these first 5 years. The heat released at the impinge of the falling materials may also serve as a catalyst to intensify the residual nuclear burning of the hydrogen-rich material

that accretes at these locations. The gravitational energy release near the poles, as well as the intense nuclear burning there, are expected to begin shortly after the eruption, when the envelope starts contracting. They also should terminate together, when the envelope finally collapses onto the *WD* surface.

6 SUMMARY

(i) Time resolved photometry of V4633 Sgr between 1998 and 2004 (three months to six years following the nova eruption) reveals two photometric periodicities in the LC.

(ii) The shorter periodicity, $P_1 = 180.8$ min was stable, and is identified as the orbital period of the underlying binary system.

(iii) The second periodicity has been shortened monotonically, from $P_2 = 185.6$ min a few weeks after the eruption to $P_2 = 183.9$ min five years later. We identify this periodicity with the spin of the *WD* primary in a magnetic CV, and the decrease as the manifestation of the *WD* spin-up due to the contraction of its envelope.

(iv) In 2004 the latter period was no longer detectable in the LC. In the near-synchronous scenario, this marks the final decline of the *WD* envelope and the termination of residual nuclear burning on the *WD* surface.

(v) V4633 Sgr thus seems to be the second known asynchronous polar classical nova.

ACKNOWLEDGMENTS

We are grateful to Dina Prialnik and Ofer Yaron for some very useful discussions. This work has been supported by the Israel Science Foundation.

REFERENCES

- Efron B., Tibshirani R. J. 1993, An Introduction to the Bootstrap, Chapman & Hall
- Hernanz, M., & Sala, G. 2007, ApJ, 664, 467
- Liller, W. 1998, IAU Circ., 6846, 1
- Liller, W., & Jones, A. F. 1999, Informational Bulletin on Variable Stars, 4664, 1
- Lipkin, Y., Leibowitz, E. M., Retter, A., & Shemmer, O. 2001, MNRAS, 328, 1169
- Lipkin, Y., & Leibowitz, E. M. 2004, IAU Colloq. 190: Magnetic Cataclysmic Variables, 315, 176
- Patterson, J. 1978, ApJ, 225, 954
- Schmidt, G. D., & Stockman, H. S. 1991, ApJ, 371, 749
- Staubert, R., Friedrich, S., Pottschmidt, K., Benloch, S., Schuh, S. L., Kroll, P., Splittgerber, E., & Rothschild, R. 2003, A&A, 407, 987
- Stockman, H. S., Schmidt, G. D., & Lamb, D. Q. 1988, ApJ, 332, 282
- Yaron, O., Prialnik, D., Shara, M. M., & Kovetz, A. 2005, ApJ, 623, 398
- Young, P. J., Corwin, H. G., Jr., Bryan, J., & de Vaucouleurs, G. 1976, ApJ, 209, 882